Journal of Computer Science
https://dergipark.org.tr/en/pub/bbd

ISSN,e-ISSN: 2548-1304
Volume:IDAP-2023, pp:131-142 , 2023
https://doi.org/10.53070/bbd.1350921
Research Paper

Evaluation of a steady-state visual evoked potential controlled quadcopter path using different performance measures

Kaan Delihasan*[1], Zafer İşcan[2]

[1] Department of Mechatronics Engineering, Bahcesehir University, Istanbul, Turkey

[2] Department of Electrical and Electronics Engineering, Bahcesehir University, Istanbul, Turkey

(kaan.delihasan@gmail.com, zafer.iscan@eng.bau.edu.tr)

Received:Aug.27,2023 Accepted:Sep.17,2023 Published:Oct.18,2023

Abstract— This study focuses on controlling a quadcopter system using a steady-state visual evoked potential (SSVEP)-based brain-computer interface system. In the literature, researchers report the accuracy and information transfer rate. However, these measures do not provide sufficient information about the predicted and target path similarity. The drone is expected to follow a certain square-shaped path and return to its starting position. We calculated the final and mean distances as additional outcome measures using several classifiers. The results emphasize the importance of having a balanced confusion matrix in the performance of quadcopter control and provide a more complete picture in the evaluation of the quadcopter's performance. Focusing on the relationship between classification accuracy and spatial deviation might create a new perspective for BCI-based control systems.

Keywords : *Unmanned Aerial Vehicles (UAV), Path following, Control, Brain-computer interface.*

1.Introduction

Technological advancement in neuroscience has led to a big interest in brain-computer interfaces (BCIs), which have applications in different fields such as clinical medicine, military, recreation, and so on (Meriño *et al.*, 2017). These systems have become more advanced with the utilization of virtual reality (Johnson *et al.*, 2018)(Cattan *et al.*, 2018)(Rutkowski, 2016), robotic devices (Bousseta *et al.*, 2018)(Wu *et al.*, 2008)(Victorio Yasin *et al.*, 2018)(Shao *et al.*, 2020), and brain-computer communication devices (Milekovic *et al.*, 2018)(Speier *et al.*, 2016).

As stated by the World Health Organization's report on disability, around 15% of the world's population cope with disability. 2-4 percent of these people experience notable difficulties in functioning. A major part of these difficulties comes from muscle diseases. BCIs can aid to make life easier for people in such conditions and reduce the human effort for various tasks. Optimizing these systems could minimize human effort and speed up the processes in the following years.

BCIs can detect the target neuronal activities from the human brain and use them to control devices such as computers. Our brain is as an electrical signal source and electroencephalography is the most common acquisition method to record these neuronal signals. It is a non-invasive technique for measuring electrical potentials (i.e. electroencephalogram) generated by brain electrical activity from electrodes placed on specific scalp locations (Shao *et al.*, 2020).

Electroencephalogram (EEG) is used to examine neurological activity and brain functions by sampling and measuring under a particular experimental protocol. In recent years, the advantages (e.g., easy recording, high resolution in time) of EEG helped in developing EEG-based BCI systems. With

proper preprocessing steps, feature extraction, and classification, a BCI transforms this activity into a control signal (Wu *et al.*, 2008).

There are different EEG paradigms used for BCIs. These paradigms can be classified as slow cortical potential (SCP), motor imagery (MI), oddball paradigm (P300), and steady-state visual evoked potential (SSVEP). SCPs are slow shifts of the EEG where the negative shifts mainly show the depolarization of the cortical cells, whereas positive shifts are related to cortical inhibition (Strehl *et al.*, 2006). P300 is the positive deviation in the EEG around 300 ms after the stimulus onset and it is located mainly in central to parietal channel locations (Polich, 2007). They are observed when there are deviant stimuli during a series of frequently presented standard stimuli. This phenomenon is known as the oddball paradigm (Fabiani *et al.*, 1981)(Hammer *et al.*, 2018). MI depends on the sensory-motor rhythm's modulations, which can be categorized as event-related synchronization (ERS) and desynchronization (ERD). Before and after the movement, ERD and ERS activities are lateralized, and specific brain patterns are generated for imagery movements. This can be used for MI-based classification (Kumar *et al.*, 2017)(Thomas *et al.*, 2013). SSVEPs are phase-locked responses from the visual cortex, generated by setting a person's gaze to a flickering visual stimulus such as a flashing light (Herrmann, 2001), or a reversing pattern (Bakardjian *et al.*, 2010). The signal that is recorded from the scalp under the stimuli has an increased amplitude at the flickering frequency and its harmonics (Mei *et al.*, 2020). There are several reasons to choose SSVEP-based BCI. Currently, it is the fastest BCI paradigm which has a high information transfer rate (ITR), high signal-to-noise ratio (SNR), and robustness (Mei *et al.*, 2020)(Shao *et al.*, 2020). Such a robust and fast method can be used to control different systems.

In the last few years, quadcopters have become popular as they are much more economical compared to other robotic systems. Even though they maintain a simple system architecture, they can be very handy when used correctly. There are many types of quadcopters depending on their size and shape, which makes their usage more common and practical for the desired operation. Quadcopters are appropriate for utilization in academic environments by researchers to analyze or assess innovative new ideas from various research topics such as real-time systems, robotics, flight control theory, and navigation (Rosca *et al.*, 2018). Due to its high SNR and robustness, in this study, the control of a quadcopter is provided by using an SSVEP-based BCI and simulated virtually to represent the control process in 2D space.

In most BCI studies, the emphasis has been on obtaining a high classification accuracy value and high ITR (Meriño *et al.*, 2017)(Mei *et al.*, 2020). However, depending on the desired outcome measure, some factors other than the classification accuracy can be more important. Classification accuracy is a critical factor most of the time, but this study shows that the desired outcome is not dependent only on accuracy. To emphasize this idea, a drone-based control system was selected to accomplish a two-dimensional (2D) flight scenario. The drone is expected to follow a certain square-shaped path and return to its starting position. The EEG data are classified into four different classes, each representing a movement direction for the drone (right, left, up, down). We compared the target (i.e., square) and predicted flight paths using four performance measures:

1) Overall accuracy (OA),

2) Final distance (FD) between the predicted and the target coordinates,

3) Mean distance (MD) between the predicted and the target coordinates, and

4) Information transfer rate (ITR).

These measures provide a more complete evaluation of the quadcopter's performance.

2. Methods

2.1 Dataset

The data used in the study were from the Tsinghua University BCI laboratory (Wang *et al.*, 2017). There are 35 subjects (18 males) between 17-34 years, with a mean age: 22 years. These subjects looked at 40 flickering characters in a frequency range of 8-15.8 Hz. The frequency interval was 0.2 Hz. Subject

5 has no data, and it was neglected for this study. There were six experiment blocks, and 40 trials were presented randomly in each block corresponding to 40 characters. Trials begin with a red square (target cue). This red cue shows up for 0.5 seconds on the screen. Subjects should switch their gaze to the target as quickly as possible within the required period. After the cue offset, stimuli were flickering on the screen simultaneously for 5 s. Following the stimulus, there was a brief (0.5 s) break where the screen was blank before the next trial for the comfort of the subjects. Each of these trials has a total length of 6 s. During the stimulation period, a red triangle was presented below the target to help fixate the eyes. For every block, subjects were requested to steer clear of eye blinks during the stimulation duration. To prevent eye fatigue, subjects had some rest for a couple of minutes between successive blocks.

EEG data is obtained from a Synamps2 system (Neuroscan, Inc.). Band-pass filter of the hardware was set from 0.15 Hz to 200 Hz. Sampling rate was 1000 Hz. A total of 64 channels covered the entire scalp for all attending subjects, and they were placed according to the international 10-20 system. The ground was put on the halfway between FPz and Fz channels. The reference electrode was placed on the vertex (Cz). Impedances between the electrodes and the scalp were below 10 kΩ. The electrical line noise was eliminated by a notch filter adjusted for 50 Hz. Collected data were segmented into epochs of 6 s length (-0.5 s to 5.5 s according to the stimulus onset). Afterward, the epochs are down sampled to 250 Hz. As a result, there were 1500 time points in each trial. There exist 6 trials for each stimulation frequency. Therefore, each subject has 120 trials (6 trials × 5 segments × 4 classes) with a segment length of 1 s.

2.2 EEG Preprocessing

The EEG data trials were split into five segments, each being one second, converting the first five seconds of the post-stimulus stage. Nine electrodes (Pz, PO5, PO3, POz, PO4, PO6, O1, Oz, and O2) were selected from the parieto-occipital region. These channels were shown to be sufficient to give accurate results (Bin *et al.*, 2009) and the BCI system can work in a useful yet less complex way. Selected four stimuli frequencies among others were 9 Hz, 11 Hz, 13 Hz, and 15 Hz. These frequencies were selected for control because the interval between them (2 Hz) should be high enough considering the frequency resolution of the segments (i.e., 1 Hz). A bandpass (0.53 – 40 Hz) Butterworth filter is applied to the data to filter the very low and high frequency components in the signal. After these steps, the data were ready for further operations.

2.3 Canonical Correlation Analysis

In this study, CCA was used as a feature extraction method. It is a statistical procedure that detects linear combinations between two random variables in a way that the correlation among the integrated variables is maximized (Hotelling, 1936). When the CCA method is used in SSVEP paradigms, correlation between the EEG data, and artificially generated sine-cosine harmonic signals are computed, and obtained correlation results are used as the features.

In this study, obtained correlations from CCA results are indicated as R values. Since there are four frequencies and their second harmonics with sine and cosine values, there are multiple ‘R’ outcomes consisting of two different values. This makes 16 values in total, but the maximum values were taken from these, corresponding to 8 ‘R’ (feature) values. R1 and R5 values show the results of the first and second harmonic for the 9 Hz stimulus, and similarly, R2 and R6, R3 and R7, and R4 and R8 show canonical correlations for 11, 13, and 15 Hz stimuli, respectively. In Figure 1, R values from the CCA algorithm were presented with a boxplot for all 120 trials belonging to subject #1.

As can be seen from the figure, R values that correspond to the stimulation frequencies are higher on average than the R values that correspond to the other frequencies. The classifiers that use these R values as feature vectors recognize the differences and operate accordingly.

2.4 Classification

The four classes indicate four directions, class one commands the drone to go right, class two commands the drone to go up, class three commands the drone to go left, and finally, the fourth class commands the drone to go down. The whole movement process contains a total number of 120 steps (30 segments × 4 classes). The drone starts the movement process from an origin which is defined as the (0, 0) point. The first movement task is +1 pixel on the x-axis in each step for 30 steps, the second task is +1 pixel on the y-axis in each step for 30 steps, the third task is -1 pixel on the x-axis in each step for 30 steps, and the final task is -1 pixel on the y-axis for 30 steps in each step. This means the drone

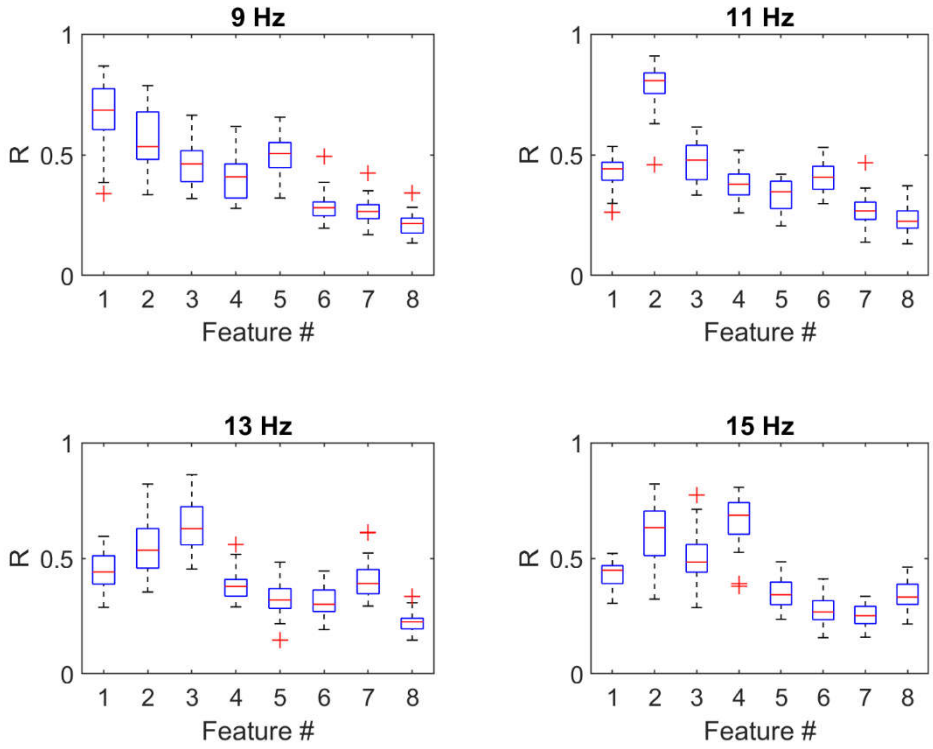

Figure 1. Boxplots of R values generated by CCA for different stimulation frequencies (Recorded from subject #1)

will follow a square-shaped path and return to its original position, which is (0, 0), but this only happens in the perfect scenario with zero classification errors.

Leave-one-out method was applied to determine classification performance which was evaluated using four outcome measures:

Overall accuracy (OA): Percentage of correctly classified directions.

Final distance (FD): Euclidean distance between the final and the starting coordinates of the drone.

Mean distance (MD): The average of instantaneous distances between the target and current coordinates of the drone.

Information Transfer Rate (ITR): This is a common metric formulated for BCI systems (Speier *et al.*, 2013). ITR converts the speed and accuracy of the specific classifier into a single metric which indicates the amount of information that is carried by the BCI in one unit of time (e.g. trials/min) (Ingel *et al.*, 2019). ITR (bits per trial) equation is given by (Wolpaw *et al.*, 2002):

$$B = log_2 N + P log_2 P + (1 - P) log_2 \frac{1-P}{N-1} \quad (1)$$

In (1), N: the number of targets, P: classification accuracy. To calculate the ITR in bits per min, B should be multiplied by the number of trials per min. In this study, there was an interval of 0.5 s for the cue and 0.5 s for the blank interval. As the stimuli interval is divided into segments of 1 s, the trial length was taken as 2 s. Therefore, the number of trials per min is determined as 30.

Three different classifiers are used for this problem: Naïve Bayes, k-Nearest Neighbor (K-NN), and Decision Tree. The performance of these three classifiers was shown before in an SSVEP-based BCI study using CCA features (Işcan and Nikulin, 2018).

2.4.1 Naïve Bayes: It is a simple probability-based classification method that measures a set of probability values obtained by calculating the frequency of each feature value in data set (Saritas, 2019). This algorithm is based on the Bayes Theorem and supposes that all variables are independent. The conditional independence supposition is infrequently accurate in real-world scenarios, so it is portrayed as Naïve, but the algorithm in general adapts rapidly in a diversity of controlled classification problems.

2.4.2 K-NN: The primary idea for k-NN relies upon calculating the distances between the test and the training data samples and the identification of the nearest training neighbors. The test data sample is determined by the class of the nearest neighbor. The k value shows the number of nearest neighbors. It is the main parameter for the classifier that directly affects the classification accuracy (Ali *et al.*, 2019).

2.4.3 Decision Tree: These sequential models perform a sequence of tests, where a numeric attribute is compared to a threshold value, or a nominal attribute is compared to a set of possible values. The goal of this algorithm is to derive or reveal patterns in the data. It does as such by figuring out which tests best separate the instances into different classes. Finally, a tree structure is formed concerning these classes (Kotsiantis, 2013).

2.5 Statistical Tests

For each of the performance measures, a one-way analysis of variance (ANOVA) is performed to determine whether the outputs from different classifiers share a common mean or not. We also performed t-tests for pair-wise comparisons.

2.6 The Quadcopter Model

Quadcopters are mobile robots that can fly in 3D space. They have six degrees of freedom. The quadcopter model used in this project is a Parrot Mini Drone. This drone has a built-in model in MATLAB, Simulink. Simulink is a block diagram-based platform that allows the model-based design to support simulations, automatic code generations, and testing. The brain signals are processed in MATLAB and then implemented in Simulink to construct the BCI environment.

The drone can move left, right, up, and down. The drone has four actuators, and these movements are provided by enhancing these four actuators in the desired way. In this project, the movement is analyzed in 2D space like a bird's-eye view to observe the control system's performance. Each of the four actuators has a motor attached to them. These motors are adjusted to spin in a suitable combination concerning each other, which causes the drone to accomplish the desired movement task. The opposite motors must spin in the same direction and opposite from the other motors to ensure that different motions will not affect each other. The control system must be constructed according to the desired task of the quadcopter, and with the help of knowledge of the system states. In this study, communication between the quadcopter control system and SSVEP activity is performed in MATLAB R2021b software.

3 Results

In Figures 2, 3, and 4, the pathways of the drone can be seen for the perfect classification (red square) scenario where the drone goes back to the initial coordinates and for the individual pathways of each subject (blue lines) using Naïve Bayes, Decision Tree, and K-NN classifiers, respectively. In Table 1, average overall accuracy (OA), mean distance (MD), and final distance (FD) values are presented.

Table 1. Performance measures of the classification of drone directions (mean ± standard error)

	Naïve Bayes	Decision Tree	K-NN
Overall Accuracy (%)	89.95 ± 1.62	81.76 ± 2.04	88.70 ± 1.82
Mean Distance (pixel)	4.44 ± 0.62	6.59 ± 0.77	4.28 ± 0.61
Final Distance (pixel)	3.80 ± 0.44	5.54 ± 0.75	5.75 ± 0.80
ITR (bits/min)	43.07 ± 2.10	30.77 ± 2.26	39.36 ± 2.25

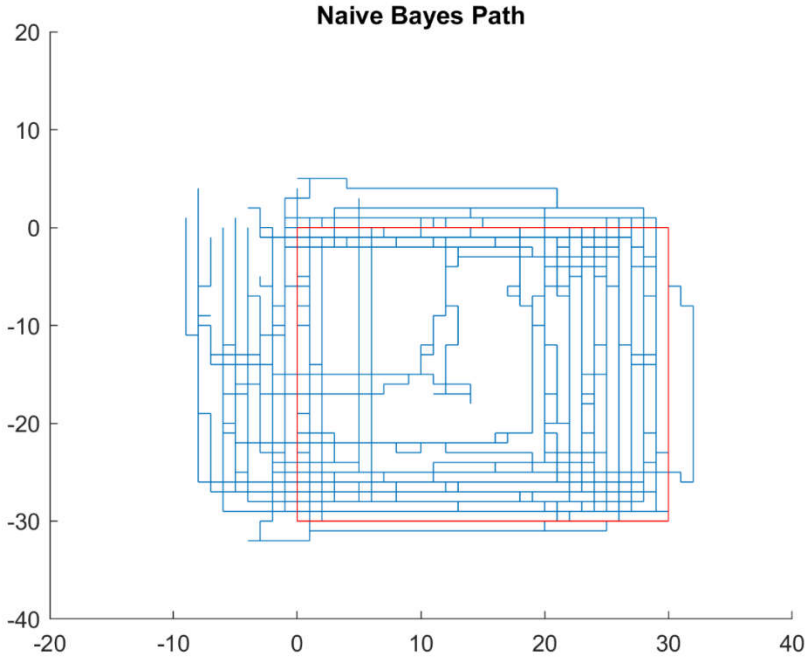

Figure 2. Pathway of all subjects (blue lines) vs. perfect scenario (Naïve Bayes)

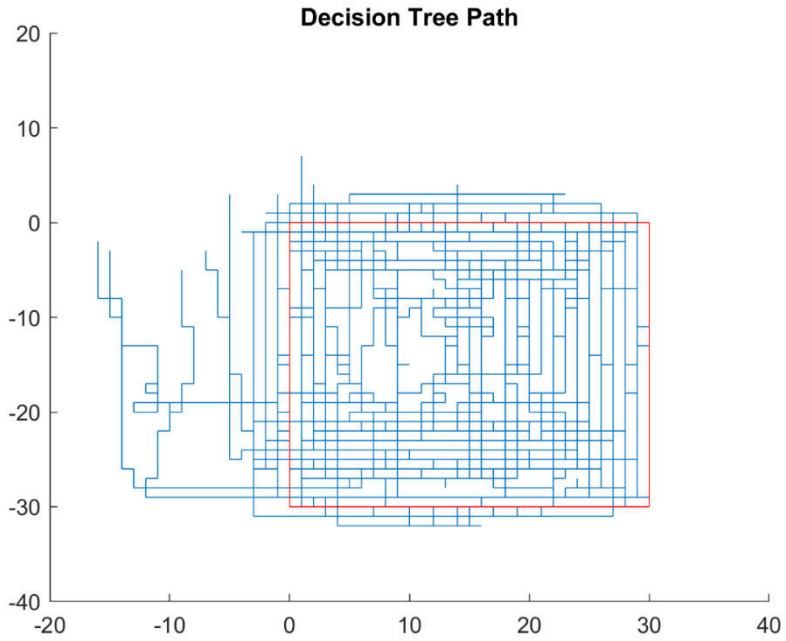

Figure 3. Pathway of all subjects (blue lines) vs. perfect scenario (Decision Tree)

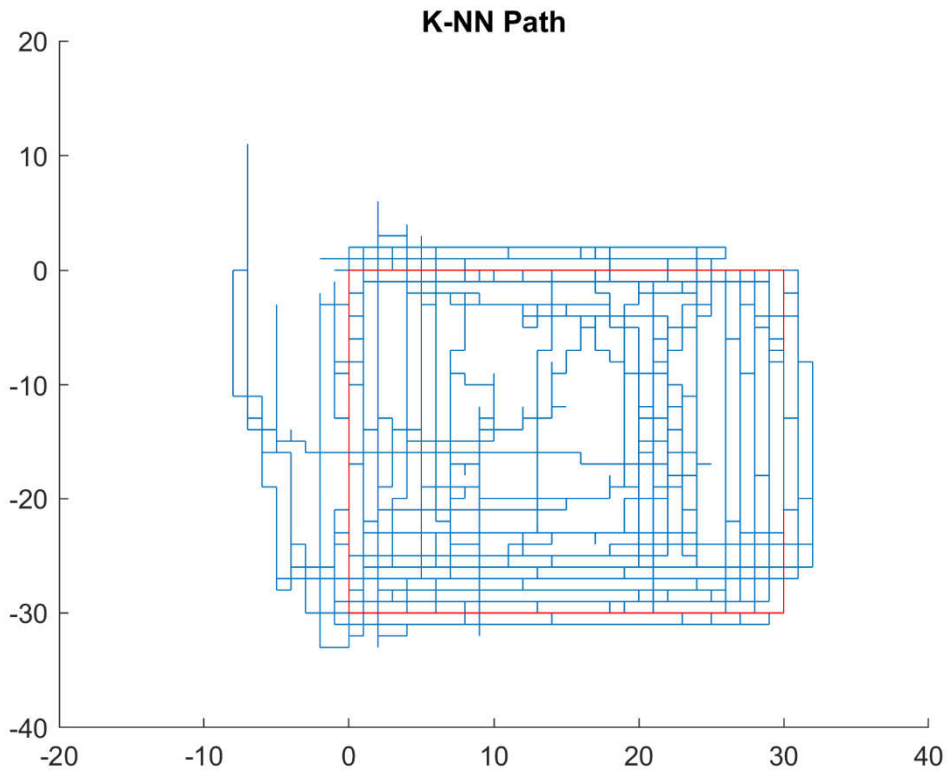

Figure 4. Pathway of all subjects (blue lines) vs. perfect scenario (K-NN)

The distribution of overall accuracy values (%) can be observed in Figure 5 as boxplots.

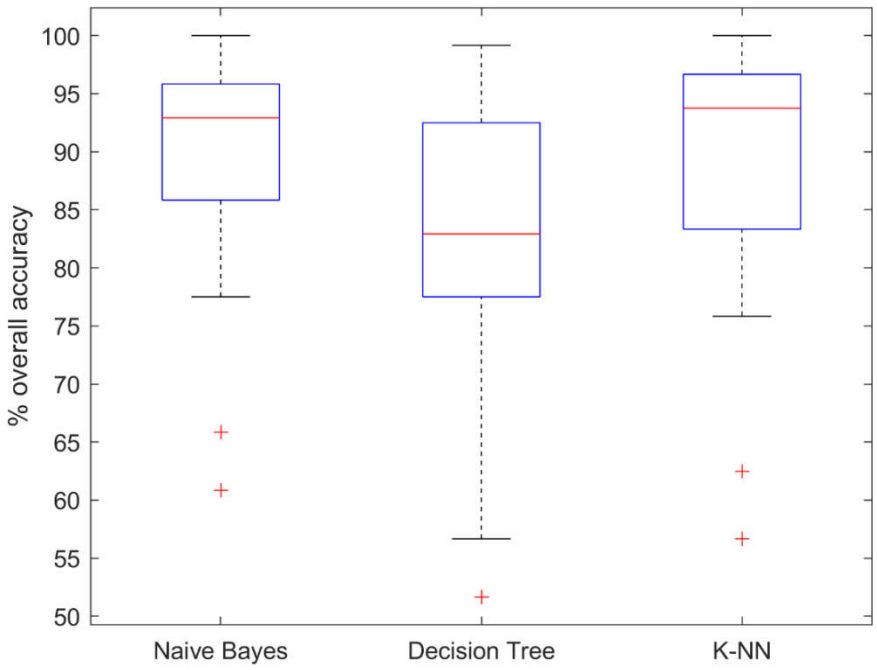

Figure 5. Boxplots of all 34 subjects' overall accuracy results for Naïve Bayes, Decision Tree, and K-NN, respectively.

The average overall accuracy (OA) ± standard error for all 34 subjects is measured as 89.95 ± 1.62, 81.76 ± 2.04, and 88.70 ± 1.82, using Naïve Bayes, Decision Tree, and K-NN, respectively. One-way ANOVA showed that the differences among group means are significant ($p < 0.01$). Multiple comparisons showed that Naïve Bayes and K-NN overall accuracies were significantly higher than the Decision Tree with a $p < 0.01$ and $p < 0.05$, respectively. The distribution of the mean and the final distance values can be observed in Figure 6 and Figure 7, respectively.

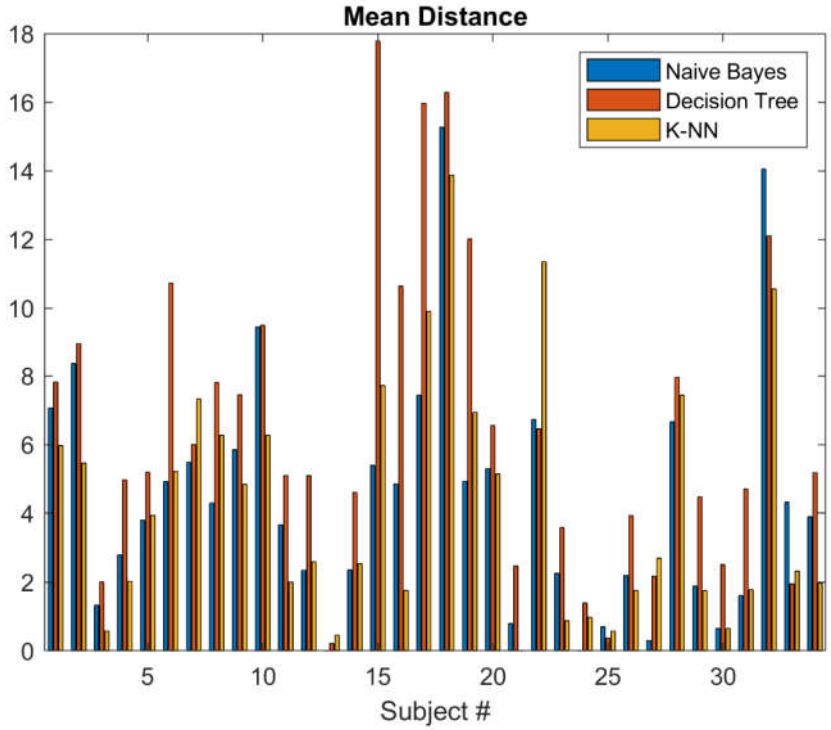

Figure 6. Distribution of the mean distance values across subjects for each classifier

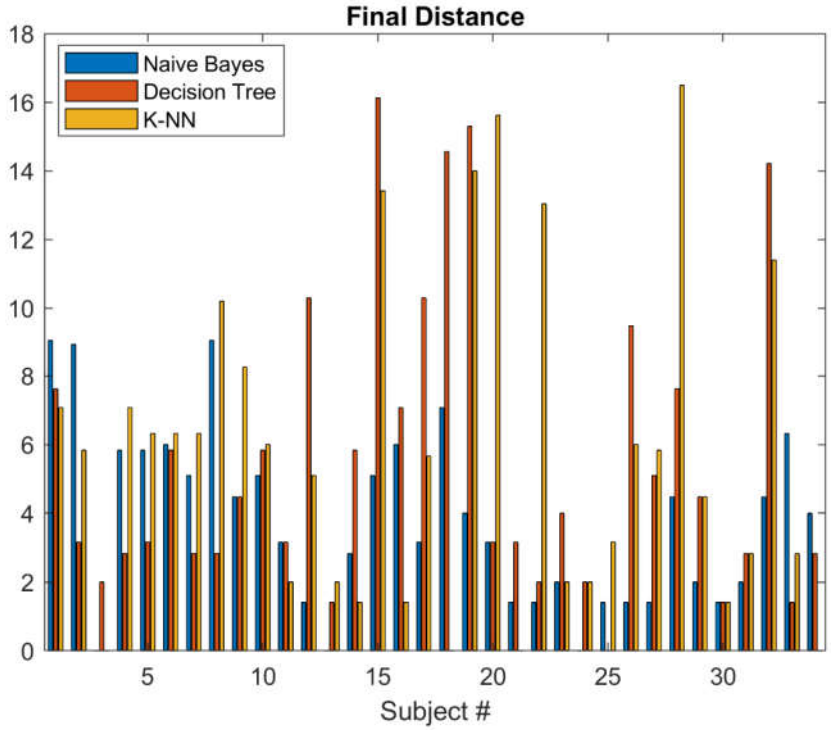

Figure 7. Distribution of the final distance values across subjects for each classifier

The mean distance (MD) ± standard error in pixels for all 34 subjects is measured as 4.44 ± 0.62, 6.59 ± 0.77, and 4.28 ± 0.61 for Naïve Bayes, Decision Tree, and K-NN, respectively. One-way ANOVA showed that the differences among group means are significant ($p < 0.05$). Multiple comparisons showed that mean distance values were significantly ($p < 0.05$) lower in K-NN than in the Decision Tree classifier. The final distance (FD) ± standard error in pixels for all 34 subjects is measured as 3.80 ± 0.44, 5.54 ± 0.75, and 5.75 ± 0.80 for the Naïve Bayes, Decision Tree, and K-NN, respectively. One-way ANOVA didn't show a difference among groups.

For the Naïve Bayes classification, subjects 13 and 24 had an overall accuracy value of 100%. These subjects had final distance and mean distance values of zero pixels as expected. Subject 3 also had a final distance value of zero pixels with an overall accuracy value of 94.17%. This subject had a mean distance value of 1.33 pixels.

For Decision Tree classification, subjects 13 and 25 had an overall accuracy value of 99.17% and 98.33%, respectively. These subjects had a final distance value of 1.41 pixels and 0 pixels, respectively. They had a mean distance value of 0.21 pixels and 0.37 pixels, respectively.

Finally, for K-NN classification, subjects 21 and 30, had an overall accuracy value of 100% and 99.17%, respectively. These subjects had a final distance value of 0 pixels and 1.41 pixels, respectively. They had a mean distance value of 0 pixels and 0.65 pixels, respectively. Subjects 3, 18, and 34 also had a final distance value of zero pixels with an overall accuracy value of 96.67%, 56.67%, and 95%, respectively. These subjects had a mean distance value of 0.58, 13.87, and 1.97 pixels, respectively. The confusion matrix for subject 18 can be seen in Figure 8.

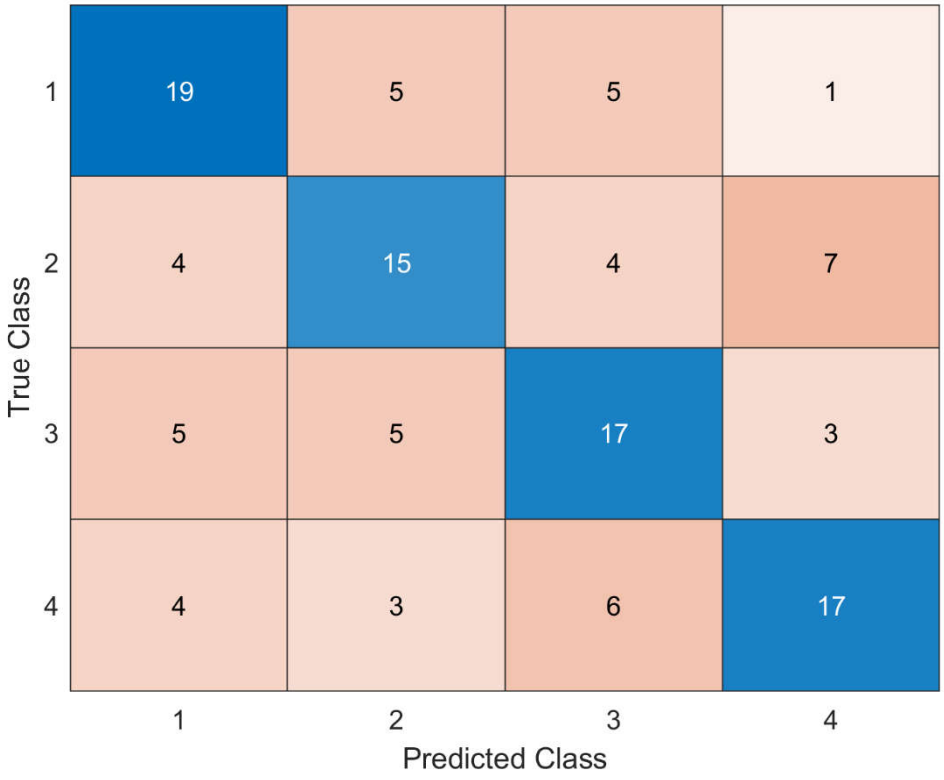

Figure 8. Confusion matrix for the K-NN classification for subject #18

Information transfer rate (ITR) ± standard error was calculated in terms of bits/min as 43.07 ± 2.10, 30.77 ± 2.26, and 39.36 ± 2.25 for Naïve Bayes, Decision Tree, and K-NN, respectively. One-way ANOVA showed that the differences among group means are significant ($p < 0.005$). Multiple comparisons showed that Naïve Bayes and K-NN ITR values were significantly higher than the Decision Tree ($p < 0.005$ and $p < 0.05$, respectively).

4 Discussion

Traditional machine learning classifiers were selected for this project because they are simple and efficient enough for this control system. Better accuracy values could be achieved with more advanced classifiers. However, the importance of this study is to show that higher overall accuracy does not necessarily mean better outcomes, as shown in the results section. Here, we evaluated the drone's path with three different classifiers using four outcome measures. Depending on the selected performance measure, the difference in classifiers can be significant or insignificant. If an unbiased confusion matrix is to be obtained, then the final distance to the desired location can be very small even though the subject has low overall accuracy (See Figure 8). If the confusion matrix obtained is not well balanced, then the final location of the drone will be further away from the desired point even though the subject has a high overall accuracy value. Therefore, it is important to evaluate the relationship between classification accuracy and distance measures. Depending on the application, the mean or final distance can be more important than the overall accuracy or ITR values.

Here we focused on a single 2D flight scenario where the quadcopter returned to its starting position. Depending on the flight scenario the relationship between the accuracy and the distance measures can vary.

5 Conclusion

This study proposes an SSVEP-based BCI control system for a quadcopter in 2D space. Results show that the quadcopter can accurately receive necessary commands and complete the movement process. Focusing on the relation between accuracy and distance might create a new perspective for BCI-based control systems. Therefore, this research could open doors for future projects concerning the control of a quadcopter or a similar robot with SSVEP-based BCIs. As a future project, the 3D simulation and movement process of a drone could be investigated. If the class number is increased from 4 to 6, then the drone could be visualized in 3D space with 6 degrees of freedom in xyz plane. Optimal maneuvers with minimum delay and maximum smoothness for such systems could also be investigated.

In the future, these systems might be used to control vehicles without the existence of a pilot or a human being, or they might be used to reduce physical fatigue in different situations. Disabled people can complete their daily tasks with the assistance of these systems, i.e., with attached components, they can fly a quadcopter to do grocery shopping, they can see and travel the outside world without having to move their muscles with an attached camera, or they can entertain themselves by playing a specific game designed for such systems. These tasks can be extended dramatically concerning the growth in BCIs. With the development and evolution of BCI-based studies, research, and projects, we will see remarkable changes in our lives in the future and these changes will be beneficial for our quality of life.

References

Ali, N., Neagu, D. and Trundle, P. (2019), "Evaluation of k-nearest neighbour classifier performance for heterogeneous data sets", *SN Applied Sciences*, Springer Nature, Vol. 1 No. 12, doi: 10.1007/s42452-019-1356-9.

Bakardjian, H., Tanaka, T. and Cichocki, A. (2010), "Optimization of SSVEP brain responses with application to eight-command Brain-Computer Interface", *Neuroscience Letters*, Vol. 469 No. 1, pp. 34–38, doi: 10.1016/j.neulet.2009.11.039.

Bin, G.Y., Gao, X.R., Yan, Z., Hong, B. and Gao, S.K. (2009), "An online multi-channel SSVEP-based brain-computer interface using a canonical correlation analysis method", *J Neural Eng.*, Vol. 6, doi: 10.1088/1741-2560/6/4/046002.

Bousseta, R., El Ouakouak, I., Gharbi, M. and Regragui, F. (2018), "EEG Based Brain Computer Interface for Controlling a Robot Arm Movement Through Thought", *IRBM*, Elsevier Masson SAS, Vol. 39 No. 2, pp. 129–135, doi: 10.1016/j.irbm.2018.02.001.

Cattan, G., Mendoza, C., Andreev, A. and Congedo, M. (2018), "Recommendations for integrating a

P300-based brain computer interface in virtual reality environments for gaming", *Computers*, doi: 10.3390/computers7020034.

Fabiani, M., Gratton, G., Karis, D. and Donchin, E. (1981), "Definition, Identification, and Reliability of Measurement of the P300 Component of the Event-Related Brain Potential", *Advances in Psychophysiology*, Vol. 2 No. 3, pp. 1–78.

Hammer, E.M., Halder, S., Kleih, S.C. and Kübler, A. (2018), "Psychological predictors of visual and auditory P300 Brain-Computer Interface performance", *Frontiers in Neuroscience*, Frontiers Media S.A., Vol. 12 No. MAY, doi: 10.3389/fnins.2018.00307.

Herrmann, C.S. (2001), "Human EEG responses to 1-100 Hz flicker: Resonance phenomena in visual cortex and their potential correlation to cognitive phenomena", *Experimental Brain Research*, Vol. 137 No. 3–4, doi: 10.1007/s002210100682.

Hotelling, H. (1936), "Relations between two sets of variates", *Biometrika*, Vol. 28, doi: 10.1093/biomet/28.3-4.321.

Ingel, A., Kuzovkin, I. and Vicente, R. (2019), "Direct information transfer rate optimisation for SSVEP-based BCI", *Journal of Neural Engineering*, IOP Publishing, Vol. 16 No. 1, p. 16016, doi: 10.1088/1741-2552/aae8c7.

Işcan, Z. and Nikulin, V.V. (2018), "Steady state visual evoked potential (SSVEP) based brain-computer interface (BCI) performance under different perturbations", *PLoS ONE*, Vol. 13 No. 1, doi: 10.1371/journal.pone.0191673.

Johnson, N.N., Carey, J., Edelman, B.J., Doud, A., Grande, A., Lakshminarayan, K. and He, B. (2018), "Combined rTMS and virtual reality brain-computer interface training for motor recovery after stroke", *Journal of Neural Engineering*, Institute of Physics Publishing, Vol. 15 No. 1, doi: 10.1088/1741-2552/aa8ce3.

Kotsiantis, S.B. (2013), "Decision trees: A recent overview", *Artificial Intelligence Review*, doi: 10.1007/s10462-011-9272-4.

Kumar, S., Mamun, K. and Sharma, A. (2017), "CSP-TSM: Optimizing the performance of Riemannian tangent space mapping using common spatial pattern for MI-BCI", *Computers in Biology and Medicine*, Elsevier Ltd, Vol. 91, pp. 231–242, doi: 10.1016/j.compbiomed.2017.10.025.

Mei, J., Xu, M., Wang, L., Ke, Y., Wang, Y., Jung, T.P. and Ming, D. (2020), "Using SSVEP-BCI to Continuous Control a Quadcopter with 4-DOF Motions", *Proceedings of the Annual International Conference of the IEEE Engineering in Medicine and Biology Society, EMBS*, Vol. 2020-July, doi: 10.1109/EMBC44109.2020.9176131.

Meriño, L., Nayak, T., Kolar, P., Hall, G., Mao, Z., Pack, D.J. and Huang, Y. (2017), "Asynchronous control of unmanned aerial vehicles using a steady-state visual evoked potential-based brain computer interface", *Brain-Computer Interfaces*, Taylor and Francis Ltd., Vol. 4 No. 1–2, pp. 122–135, doi: 10.1080/2326263X.2017.1292721.

Milekovic, T., Sarma, A.A., Bacher, D., Simeral, J.D., Saab, J., Pandarinath, C., Sorice, B.L., *et al.* (2018), "Stable long-term BCI-enabled communication in ALS and locked-in syndrome using LFP signals", *Journal of Neurophysiology*, Vol. 120 No. 1, doi: 10.1152/jn.00493.2017.

Polich, J. (2007), "Updating P300: An integrative theory of P3a and P3b", *Clinical Neurophysiology*, October, doi: 10.1016/j.clinph.2007.04.019.

Rosca, S., Leba, M., Ionica, A. and Gamulescu, O. (2018), "Quadcopter control using a BCI", *IOP Conference Series: Materials Science and Engineering*, Vol. 294, Institute of Physics Publishing, doi: 10.1088/1757-899X/294/1/012048.

Rutkowski, T.M. (2016), "Robotic and virtual reality BCIs using spatial tactile and auditory oddball paradigms", *Frontiers in Neurorobotics*, doi: 10.3389/fnbot.2016.00020.

Saritas, M.M. (2019), "Performance Analysis of ANN and Naive Bayes Classification Algorithm for

Data Classification", *International Journal of Intelligent Systems and Applications in Engineering*, International Journal of Intelligent Systems and Applications in Engineering, Vol. 7 No. 2, pp. 88–91, doi: 10.18201/ijisae.2019252786.

Shao, L., Zhang, L., Belkacem, A.N., Zhang, Y., Chen, X., Li, J., Liu, H., *et al.* (2020), "EEG-Controlled Wall-Crawling Cleaning Robot Using SSVEP-Based Brain-Computer Interface", *Journal of Healthcare Engineering*, Hindawi Limited, Vol. 2020, doi: 10.1155/2020/6968713.

Speier, W., Arnold, C. and Pouratian, N. (2013), "Evaluating True BCI Communication Rate through Mutual Information and Language Models", *PLoS ONE*, Vol. 8 No. 10, doi: 10.1371/journal.pone.0078432.

Speier, W., Arnold, C. and Pouratian, N. (2016), "Integrating language models into classifiers for BCI communication: A review", *Journal of Neural Engineering*, doi: 10.1088/1741-2560/13/3/031002.

Strehl, U., Leins, U., Goth, G., Klinger, C., Hinterberger, T. and Birbaumer, N. (2006), "Self-regulation of slow cortical potentials: A new treatment for children with attention-deficit/hyperactivity disorder", *Pediatrics*, Vol. 118 No. 5, doi: 10.1542/peds.2005-2478.

Thomas, E., Fruitet, J. and Clerc, M. (2013), "Combining ERD and ERS features to create a system-paced BCI", *Journal of Neuroscience Methods*, Vol. 216 No. 2, doi: 10.1016/j.jneumeth.2013.03.026.

Victorio Yasin, T., Pasila, F. and Lim, R. (2018), "A Study of Mobile Robot Control using EEG Emotiv Epoch Sensor", *MATEC Web of Conferences*, Vol. 164, EDP Sciences, doi: 10.1051/matecconf/201816401044.

Wang, Y., Chen, X., Gao, X. and Gao, S. (2017), "A Benchmark Dataset for SSVEP-Based Brain-Computer Interfaces", *IEEE Transactions on Neural Systems and Rehabilitation Engineering*, Vol. 25 No. 10, doi: 10.1109/TNSRE.2016.2627556.

Wolpaw, J.R., Birbaumer, N., McFarland, D.J., Pfurtscheller, G. and Vaughan, T.M. (2002), "Brain-computer interfaces for communication and control", *Clin. Neurophysiol.*, Vol. 113, doi: 10.1016/S1388-2457(02)00057-3.

Wu, L.W., Liao, H.C., Hu, J.S. and Lo, P.C. (2008), "Brain-controlled robot agent: An EEG-based eRobot agent", *Industrial Robot*, Vol. 35 No. 6, pp. 507–519, doi: 10.1108/01439910810909501.